Int. J. Heat Mass Transfer. Vol. 15, pp. 2427–2445. Pergamon Press 1972. Printed in Great Britain

FILM BOILING OF WATER AND AN AQUEOUS BINARY MIXTURE

S. J. D. VAN STRALEN, C. J. J. JOOSEN† and W. M. SLUYTER
Heat Transfer Section, University of Technology, Eindhoven, Netherlands

(*Received* 29 *December* 1971)

Abstract—Film boiling of water and of an aqueous binary mixture with a more volatile component (4·1 wt % 2-butanone) has been studied on a horizontal, electrically heated platinum wire with a diameter of 200 μm.

The most important experimental result is the reduction of the direct vapour production at the film in the mixture, which accounts to only 53 per cent of the heat flux, in contrast to a value of 95 per cent in pure liquids. Also, the heat transfer coefficient in the mixture is increased up to a factor of 1·8 at burnout in comparison to water.

The curious behaviour of the mixture is attributed to mass diffusion: a local exhaustion of the more volatile component in the liquid at the film interface causes an additional heat flow into the bulk liquid.

NOMENCLATURE

b,	growth paramter, $-$ *in* [1/s];
c,	wave velocity on liquid–vapour interface, n/m [m/s];
c_p,	specific heat at constant pressure [J/kg deg C];
C,	asymptotic growth constant for free bubbles [m/s$^{\frac{1}{2}}$ deg C];
d,	thickness of vapour film [m];
D,	mass diffusivity of more volatile component in less volatile component [m^2/s];
D_w,	diameter of heating wire [m];
e,	base of natural logarithms, 2·718...;
f,	fraction of heating area covered by vapour columns at burnout;
g,	gravitational acceleration [m/s^2];
h,	heat-transfer coefficient [W/m^2 deg C];
i,	imaginary number, $(-1)^{\frac{1}{2}}$;
k,	thermal conductivity [W/m deg C];
l,	specific enthalpy difference between superheated or saturated vapour and liquid at saturation temperature [J/kg];
L,	center distance between neighbouring bubbles at interface [m];
L_w,	length of heating wire [m];
m,	wave number $2\pi/\lambda$, [1/m];
n,	angular frequency [1/s];
q,	heat flux density [W/m^2];
q^*,	contribution to heat flux density due to direct vapour production at film [W/m^2];
q',	radiant heat flux density [W/m^2];
R,	equivalent bubble radius [m];
R_1,	equivalent bubble radius at departure [m];
R_w,	radius of heating wire, $D_w/2$, [m];
t,	time [s];
t_1,	adherence time of bubble [s];
t_2,	waiting time between succeeding bubbles [s];
Δt,	time inverval in equation (19) [s];
T,	absolute boiling temperature [K];
T_w,	absolute temperature of heating wire [K];
v,	velocity [m/s];
x,	abscissa parallel to wire axis [m];
x_0,	mass fraction of more volatile component in original liquid in binary mixture;

---

† Present address: National Aerospace Laboratory, Amsterdam, Netherlands.

z,	ordinate of harmonic wave on liquid–vapour interface [m];
z_0,	amplitude of harmonic wave [m].

Greek letters

α,	shear stress factor at interface;
β,	positive integer relating prominence distance to dominant wavelength;
ε,	emissivity;
η,	dynamic viscosity [kg/sm];
θ_0,	average wire superheating [deg C];
$\theta_{0,1}$,	local liquid superheating near interface [deg C];
κ,	constant of proportionality in equation (4);
λ,	wavelength [m];
λ_c,	critical wavelength [m];
λ_d,	dominant or most dangerous wavelength [m];
ν,	bubble frequency, $1/(t_1 + t_2)$, [1/s];
ρ,	density [kg/m^3];
σ,	surface tension constant between liquid and vapour [kg/s^2];
τ,	bubble period, $t_1 + t_2$, $1/\nu$, [s].

Subscripts

1,	value for liquid;
2,	value for vapour;
c,	applies to critical wavelength;
d,	applies to dominant wavelength;
max,	maximum value at nucleate boiling peak flux or at burnout in film boiling;
w,	value for heating wire.

1. SURVEY ON THE MECHANISM OF NUCLEATE BOILING IN PURE LIQUIDS AND BINARY MIXTURES

In NUCLEATE boiling of binary mixtures on electrically heated wires, a curious coincidence has been observed previously by Van Wijk, Vos and Van Stralen [1], and by Van Stralen [2, 3] of a maximal peak flux density and a minimal bubble growth rate at the same (low) concentration of the more volatile component.

The slowing down of bubble growth is due to the influence of mass diffusion of the more volatile component towards the bubble boundary, causing an increase in dew point of the vapour. This limits the analogous heat diffusion, originally controlled by the liquid superheating [1–7]. The most favourable concentration can be derived from equilibrium data only.

Van Stralen's [8–10] "relaxation microlayer" theory explains the above mentioned "boiling paradox" quantitatively. This paradox occurs more generally in any boiling system, which is characterized by the action of small bubbles generated at high frequencies. According to this theory, nucleate boiling is described as a relaxation phenomenon of the superheated thermal boundary layer, which is periodically pushed away from the wall due to the rapid initial growth of succeeding bubbles on nuclei.

A subsequent superheating of saturated liquid flowing to the surroundings of the nucleus occurs during the waiting (or delay) time between the detachment of a bubble and the generation of the succeeding bubble. The corresponding (initially high) local heat flux density is usually mainly determined by liquid properties. Expressions for the adherence and delay times, the bubble frequency, the departure radius, the vaporized mass and diffusion fractions at the heating surface, and the peak flux in dependence on concentration could thus be derived.

Ultimately, the action of the vapour bubbles could be described as an augmentation of convective heat transfer. Van Stralen and Sluyter [11] verified experimentally the common physical background underlying the various bubble growth theories and the "relaxation microlayer" model. For this purpose, local temperature fluctuations recorded with the hot junction of a thin-wired thermocouple, have been synchronized with high-speed motion pictures of vapour bubbles.

2. RESULTS FOR THE SYSTEM WATER–2-BUTANONE IN NUCLEATE BOILING AT ATMOSPHERIC PRESSURE

The binary system water–2-butanone (methylethylketone)—for which equilibrium data at constant pressure are available in the literature—has been studied most extensively [12, 6, 7]. At the most favourable composition, i.e. 4·1 wt % 2-butanone (the more volatile component), an increase in the nucleate boiling "peak" or "critical" flux occurs to a value of 172 × 10^4 W/m^2 in comparison to 72 × 10^4 W/m^2 for water (Figs. 1 and 2), and to 36 × 10^4 W/m^2 for 2-butanone. These values were observed on horizontal platinum wires with a diameter of 2·00 × 10^{-4} m. On vertical wires, the peak flux in the mixture has been decreased with only 10 per cent in comparison to 30 per cent in water [13]; this more favourable behaviour of the mixture has been attributed to the Marangoni-effect (a surface tension effect), which diminishes bubble coalescence in the mixture.

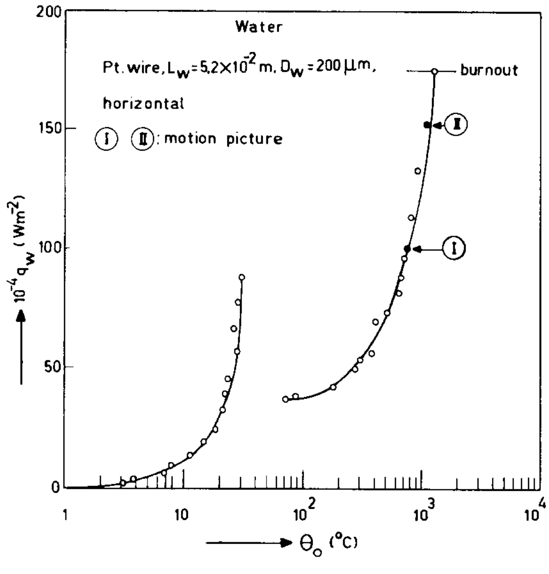

FIG. 1. Water. Boiling curve for convection, nucleate boiling and film boiling up to burnout. (I) and (II) indicate the simultaneous recording of a high-speed motion picture, cf. Figs. 3 and 4, respectively.

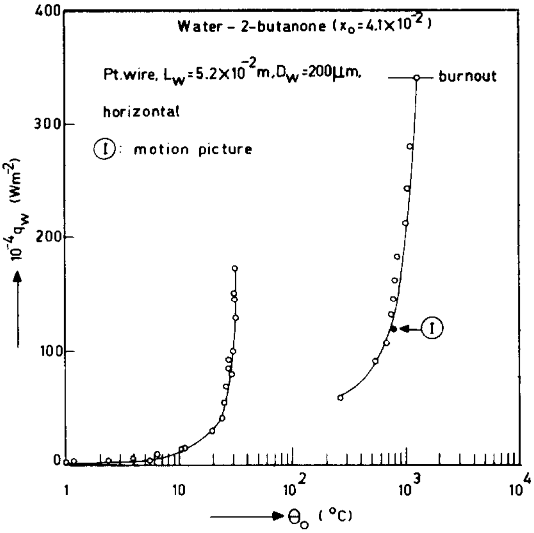

FIG. 2. 4·1 wt % 2-butanone. Boiling curve for convection, nucleate boiling and film boiling up to burnout. (I) indicates the simultaneous recording of a high-speed motion picture, cf. Fig. 5.

Both the theoretical and experimental values of the asymptotic growth constant, $C = R(t)/\theta_0 t^{\frac{1}{2}}$, for free bubbles in the mixture is reduced to 0·25 times the corresponding value in water [6, 7, 10]. This reduction shows that the increase in dew point of the vapour in the bubbles equals 75 per cent of the liquid superheating. In accordance with this, the experimental average bubble departure radius in nucleate boiling decreases from 9·2 × 10^{-4} m in water to 3·4 × 10^{-4} m in the mixture.

The maximal density of active nuclei at the peak flux amounts to approximately 400 × 10^4 m^{-2} in the mixture, and to 70 × 10^4 m^{-2} in water; the average bubble frequency to 175 s^{-1} and 70 s^{-1}, respectively [8]. The maximal direct vapour formation on the heating wire at the critical flux in nucleate boiling corresponds to a heat flux density contribution of 30 × 10^4 W/m^2, both in water and the mixture; apparently, however, at two greatly different peak flux densities.

Possibly, a new criterion for the departure from nucleate boiling can be based on this remarkable situation, which is giving a suitable starting point for studying both film boiling and the transition region, cf. Sections 3 and 10.2.

3. COMPARISON WITH ZUBER'S THEORY BASED ON HELMHOLTZ INSTABILITY

Also, this criterion seems to be consistent with Zuber's [14–16] derivation of an expression of the critical flux, which is based on the incipience of a Helmholtz instability distorting the stable capillary wave character of the interface between the upward vapour flow (velocity: v_2) and the corresponding downward liquid flow (velocity: v_1). Hydrodynamic stability requires, that

$$v_2 = -\frac{\rho_1}{\rho_2} v_1 < \left[\frac{\rho_1 \sigma m_c}{\rho_2(\rho_1 + \rho_2)}\right]^{\frac{1}{2}}, \tag{1}$$

where the critical wave number m_c depending on the critical wavelength λ_c is given by the following expression, cf. equation (8):

$$m_c = \frac{2\pi}{\lambda_c} = \left[\frac{g(\rho_1 - \rho_2)}{\sigma}\right]^{\frac{1}{2}}. \tag{2}$$

Zuber relates the peak flux density of a pure liquid on a flat heating plate to v_2 as follows:

$$q_{w,\max} = \frac{\pi}{24}\rho_2 l v_2 = \frac{\pi}{24}\rho_2 l \left[\frac{\sigma g(\rho_1 - \rho_2)}{\rho_2^2}\right]^{\frac{1}{4}} \times \left[\frac{\rho_1}{\rho_1 + \rho_2}\right]^{\frac{1}{2}}. \tag{3}$$

The constant $\pi/24$ originates from the fraction occupied by the vapour columns.

A constant vapour production both in water and the investigated mixture at the peak flux implicates a nearly constant v_2 in both cases, the slight difference depending on σ and ρ_2.

Disadvantages of Zuber's model in comparison to Van Stralen's relaxation microlayer theory are: (a). the increased peak fluxes occurring in binary mixtures are not involved; (b). the convective heat flux is neglected; (c). the model is not extended to a cylindrical heating surface. On the other hand, the well-known experimental relation of Cichelli and Bonilla [17] i.e. the peak flux of pure liquids in dependence on pressure shows a maximum at 1/3 of the critical pressure, is in good agreement with equation (3).

4. SCOPE OF THE PRESENT INVESTIGATION ON FILM BOILING

The main object of the present study is to verify if the strong influence of mass diffusion, which is demonstrated in nucleate boiling of mixtures, occurs eventually also in film boiling. In connection to the previous results in nucleate boiling, emphasis is laid on the individual growth rates of bubbles generated at the separating vapour film, on the heat flux density at constant wall superheating, and on the burnout flux. The behaviour of water is compared to that of the mixture containing 4·1 wt % (i.e. 1·0 mole %) 2-butanone in water, and in some cases also to that of ethanol (more exactly: the azeotropic mixture, 96 wt % ethanol in water). Restriction has been made to investigations at atmospheric pressure.

Unconventionally for research in film boiling, the experimental programme started with high-speed cinematographic recordings* (at a rate of 3500 frames per s) of the direct vapour production at the vapour–liquid interface of the film, which surrounds the electrically, d.c.-heated horizontal platinum test wire, c.f. Section 2.

These wires (with a diameter of $2{\cdot}00 \times 10^{-4}$ m and a length of approximately 5×10^{-2} m) are immersed in a relatively large boiling vessel provided with an electrically heated bottom plate and a total-reflux condenser [1, 2, 6, 7]. They are used both as a heating surface and as a resistance thermometer.

Results on water and ethanol show that the convective liquid flow arising from the heating of the bottom plate, had no noticeable influence on the energy balance, i.e. the direct vapour

---

† These recordings at the superheatings shown in Table 1 have been carried out within 2 min to avoid a contamination (less than 1 μm) of the wire surface due to a thermal decomposition of the organic component at high superheatings. A carbon layer of 20 μm thickness is deposited during 10 min slightly below burnout conditions in the mixture, and a corresponding layer of 5 μm in ethanol.

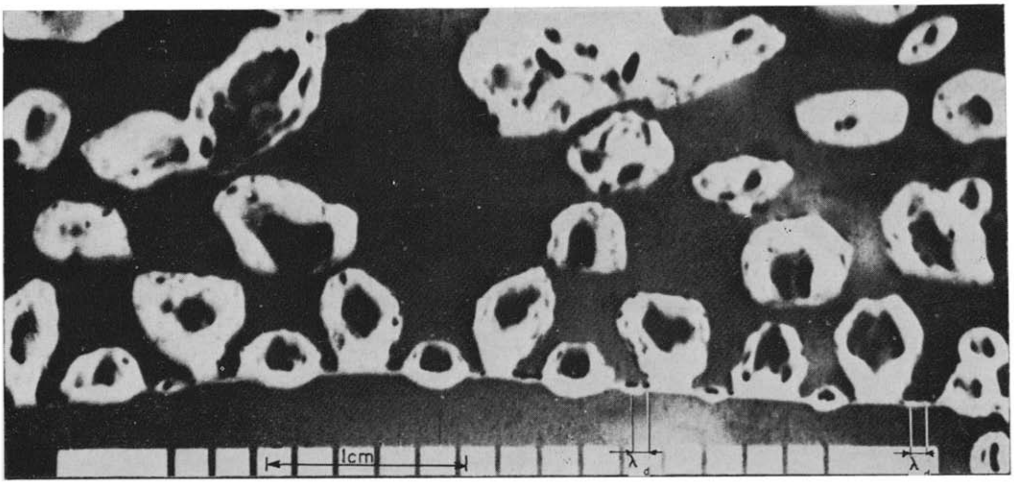

FIG. 3. Water, (I), cf. Fig. 1 and Table 1. High-speed photograph showing bubbles in film boiling at $\theta_0 = 744$°C and $q_w = 101 \times 10^4$ W/m^2. Generally, the regular pattern governed by the dominant wavelength λ_d is disturbed by coalescense of prominences and bubbles, cf. Fig. 4.

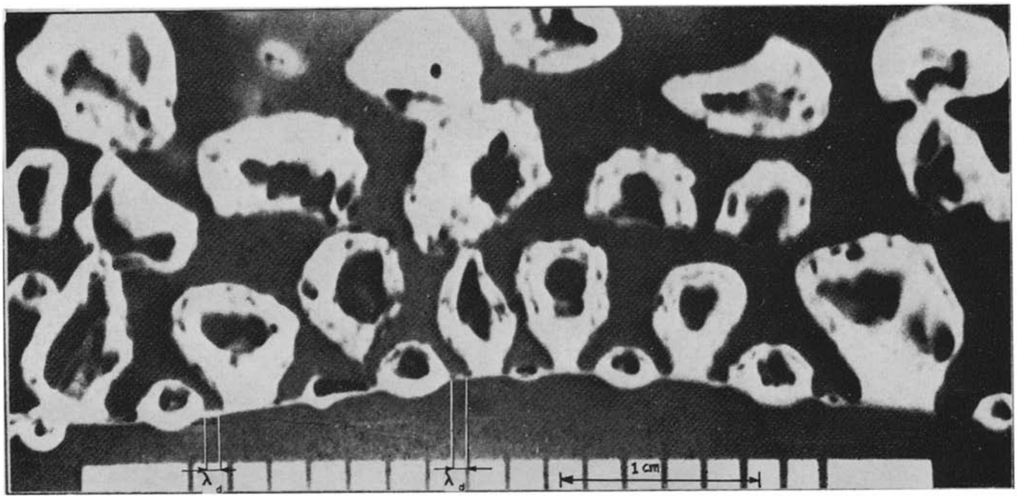

FIG. 4. Water, (II), cf. Fig. 1 and Table 1. High-speed photograph showing bubbles in film boiling at $\theta_0 = 1063$°C and $q_w = 154 \times 10^4$ W/m^2. Coalescense occurs more frequently at increasing flux, cf. Fig. 3.

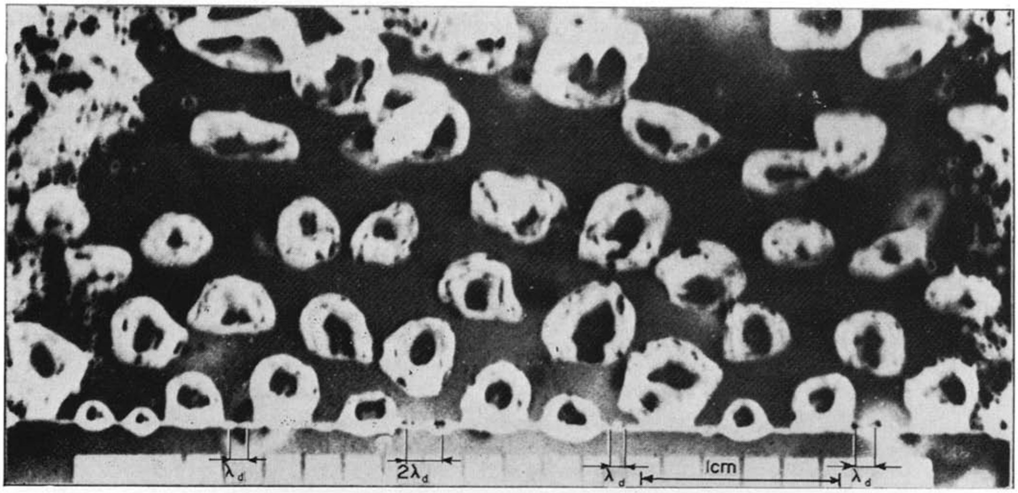

FIG. 5. 4·1 wt% 2– butanone in water, (I), cf. Fig. 2 and Table 1. High-speed photograph showing bubbles in film boiling at $\theta_0 = 788°C$ and $q_w = 123 \times 10^4$ W/m^2. The direct vapour production is reduced in comparison to water and coalescense occurs even less frequently as in water, (I).

Table 1. Survey of experimental data in film boiling at atmospheric pressure. The data for water, (I), correspond to Figs. 1, 3 and 6, the data for water, (II), to Figs. 1, 4 and 6, and the data for 4·1 wt % 2-butanone to Figs. 2, 5 and 7. Recordings of the motion pictures and the boiling curve have been synchronized

Platinum wire, horizontal electrically d.c.-heated. Length L_w = 5·2 cm, dia. D_w = 200 µm. Surface area $\pi D_w L_w$ = 0·327 cm^2.	Liquid				
	Water		Ethanol		Water–2-butanone (x_0 = 4·1 × 10^{-2})
	(I)	(II)	(I)	(II)	
Wire superheating θ_0 (°C)	744	1063	329	831	788
Heat flux density q_w (W/cm^2)	101	154	46	189	123
Direct vapour production $q_w{}^*$ (W/cm^2) equation (19)	93·6	147·1	45·1	168·2	64·7
Radiant flux density q'_w (W/cm^2) equation (20)	1·2	4·2	0·2	1·6	1·4
Relative contribution of direct vapour production $q_w{}^*/(q_w - q'_w)$	0·94	0·98	0·98	0·90	0·53
Average number of sites generating bubbles at upper side of film	16	15	21	10	17
Average density of sites for bubble generation (cm^{-2})	49	46	64	31	52
Average bubble frequency on sites $\bar{\nu}$ (s^{-1})	26	22	33	29	23
Average distance between neighbouring sites (mm)	3·06	3·25	2·36	4·73	2·84
Average bubble departure radius $\bar{R}_1$ (mm)	2·34	2·87	1·52	3·17	2·11

production at the film in pure liquids corresponds to the total heat flux (Table 1).

The experimental results for the investigated pure liquids are compared to predictions following from current theories on the mechanism of film boiling specialized to the case of horizontal heating cylinders. Generally, deviations can be attributed to the invalidity of assumptions underlying the theoretical models, which are mainly applicable only in case of low heat flux densities occurring near the minimum in the boiling curve at the Leidenfrost-point.

The observed remarkable influence of mass diffusion in film boiling of the mixture is explained qualitatively in terms of the same physical background, which underlies this process in nucleate boiling.

5. INTRODUCTION TO FILM BOILING THEORIES

In the stable region of film boiling, the heating surface and the boiling liquid are separated by a thin superheated vapour film. In general, relatively large vapour bubbles are released more or less regularly from the upper side of the vapour–liquid interface.

Common theories on film boiling of pure liquids are based on two different physical approaches:

(a) The heat transport through the vapour film is considered to be of primary importance.
(b) The heat removal from the surface is assumed to be governed by the behaviour of the bubbles, which in turn should be related to the occurrence of hydrodynamic instabilities at the vapour–liquid interface according to Taylor [18].

The former conception was presented by Bromley [19] for horizontal heating cylinders, and modified by others with the purpose of extending the limitations concerning tube diameter.

Chang [20], Zuber [14, 15] and others presented model theories for film boiling on horizontal flat plates, which are based on critical hydrodynamic stability. The validity of these models is restricted to low heat fluxes near the minimum value at the Leidenfrost-point.

Berenson [21] improved the theory by emphasizing the importance of the "most dangerous" or "dominant" wavelength λ_d instead of the "critical" wavelength λ_c, and by deriving an expression for the vapour velocity to the bubbles. His final equation for the heat transfer coefficient at the minimum is similar to Bromley's expression, but the tube diameter has been replaced by the most dangerous wavelength.

Lienhard and Wong [22] extended the validity of the hydrodynamic instability theory to the case of thin horizontal heating wires by accounting for the effect of surface tension along the curved periphery of the vapour–liquid interface in a cross-section.

Some years ago, Jordan [23] presented an extensive survey on the current theoretical predictions for film boiling in comparison to existing experimental data. Contrarily to the behaviour in nucleate boiling, the thermal properties of the heating surface seem to have no appreciable influence on film boiling. It may be worth noticing, that all common theories for film boiling assume the presence of a saturated (or uniformly subcooled) bulk liquid; the eventual existence of a thin superheated liquid layer at the vapour film boundary is rejected *a priori*. This seems to be questionable with respect to both Bromley's and Berenson's models, which assume a flow of saturated vapour (originating at the interface) through the superheated vapour film to the bubble space.

6. EXPERIMENTAL RESULTS BY OTHERS ON FILM BOILING OF BINARY MIXTURES

To the knowledge of the present authors, the only research on film boiling (on a horizontal flat plate) of miscible binary mixtures of volatile components, which is presented in the literature, has been carried out by Kautzky and Westwater [24] on the system carbon tetrachloride–Freon 113. The experimental heat flux density of CCl_4, at a constant wall superheating of 125°C, was increased with nearly 20 per cent by addition of only 1 wt % Freon, the more volatile component. The incorporation of mass diffusion in Berenson's film boiling theory is suggested to predict the behaviour of binary mixtures. However, no indication is given about the way, in which this should be established.

Dunskus and Westwater [25] observed increases in film boiling of the heat transfer coefficient up to a factor of 3 by adding 0·1 mole % of a nonvolatile additive of high molecular weight (Igepal CO-880) to isopropanol. Van Stralen [6] showed theoretically, that a slowing down of the growth rate of free vapour bubbles due to mass diffusion occurs also in case of addition of a nonvolatile component e.g. a salt.

7. THE BROMLEY THEORY

In analogy with the Nusselt [26, 27] theory for film-type condensation, Bromley [19] considered both heat conduction and radiant flux through the thin vapour film surrounding a horizontal heating cylinder in film boiling. The effect of the vapour bubbles, which are released from the upper part of the film, has been neglected. The upward vapour flow through the film is assumed to be laminar; heat removal and the corresponding vaporization occurs mainly at the lower side of the cylinder, where the film thickness is the smallest. At high superheatings of the cylinder surface, an interaction of radiant and convective flux occur, as the thickness of the film increases due to radiation. Bromley accounts the radiant flux to 75 per cent of the value calculated from the Stefan–Boltzmann law for black-body radiation, corrected for the emissivity of the cylinder material.

The resulting equation for the mean heat transfer coefficient at relatively low superheatings, where radiation can be neglected, is as follows:

$$\bar{h}_w = \frac{\bar{q}_w}{\theta_0} = \kappa \left[\frac{k_2^3 \rho_2 l(\rho_1 - \rho_2) g}{\eta_2 \theta_0 D_w} \right]^{\frac{1}{4}}. \qquad (4)$$

The numerical value of the constant in the right-hand side of equation (4) depends on the shear stresses at the heating surface and at the interface, and amounts to $\kappa = 0{\cdot}512$ for the extreme case of stagnant liquid and to $\kappa = 0{\cdot}725$ for the other extreme case of freely rising liquid exerting no frictional drag on the vapour. These values can be derived from the expression $\kappa = 0{\cdot}954/\alpha^{\frac{1}{4}}$, where, more generally, the shear stress factor α has to satisfy the condition $3 \leqslant \alpha \leqslant 12$. The average value $\kappa = 0{\cdot}62$ was taken by Bromley.

Equation (4) can be derived easily from dimensional analysis by taking $Nu = (Gr\,.\,Pr)^{\frac{1}{4}}$ for horizontal cylinders, similar to the case of natural convection. One has to substitute [28] the usual Nusselt number

$$Nu = \bar{q}_w \frac{D_w}{k_2 \theta_0} = \frac{h_w}{k_2} D_w,$$

the modified Grashof number

$$Gr = \frac{\rho_2^2}{\eta_2^2} \frac{g(\rho_1 - \rho_2)}{\rho_2} D_w^{\ 3}$$

$$= \frac{\rho_2 g(\rho_1 - \rho_2)}{\eta_2^2} D_w^{\ 3},$$

and the modified Prandtl number

$$Pr = \frac{c_{p,2}\,\eta_2}{k_2} \cdot \frac{l}{c_{p,2}\,\theta_0} = \frac{\eta_2}{k_2} \frac{l}{\theta_0};$$

here l denotes the specific enthalpy difference between superheated vapour and saturated liquid. The numerical values of the physical property constants of the vapour are evaluated at the average superheating of $\theta_0/2$.

The practical applicability of equation (4) is limited to the following range of tube diameters:

$$10^{-3}\,\mathrm{m} < D_w < \lambda_d = 2\pi \left[\frac{3\sigma}{g(\rho_1 - \rho_2)}\right]^{\frac{1}{2}}.$$

The upper limit follows from hydrodynamic instability, c.f. Section 8 and [23].

For thin heating wires below the indicated lower limit, Bromley's equation with $\kappa = 0{\cdot}62$ predicts heat fluxes which are up to an order of magnitude too low. Berenson's [21] modification (cf. Sections 5 and 8) involves a constant $\kappa = 0{\cdot}49$, if λ_d is inserted, taken from experimental results at the Leidenfrost-point on horizontal flat plates.

Pitschmann and Grigull [28] removed the lower limit of applicability of Bromley's theory to thin cylinders by removing the requirement, that the mean film thickness $\bar{d}$ should be small in comparison to the wire diameter D_w. The assumptions of laminar upward vapour flow, of heat conduction through the vapour film and of saturated liquid, are maintained.

Both the Nusselt number and the Rayleigh number $Ra = Gr.Pr$ are modified by these authors with a radiation factor and a Smoluchowski-factor to account for the radiant flux and for the decrease of the effective superheating (which increases the heat transfer coefficient), respectively. The latter effect is due to a temperature jump between the heating surface and the adjacent vapour. This follows from gas kinetics and is of practical importance only if the mean free path of the vapour molecules and the film thickness are of the same order of magnitude, i.e. in case of thin heating wires in combination with low pressure; cf. the mean free path at atmospheric pressure and at room temperature of a number of gases, which is of the order of 10^{-7} m [29].

Pitschmann and Grigull's final equation fits to a large number of experimental data on thin wires, but has the disadvantage of the introduction of three empirical constants and three exponents ranging from 0·08 and 0·4. It seems to be difficult to decide about an eventual preference to be given to this treatment or to Lienhard and Wong's [22], where the circumferential surface tension introduces a strong effect of wire diameter, c.f. Sections 5, 8 and 9.

8. THE HYDRODYNAMIC INSTABILITY THEORY

8.1 *Survey*

The following generalized expression [23, 30, 31] is introduced for the wave velocity c of harmonic waves (first-order perturbation) with small amplitude z_0: $z = z_0\,e^{-int} \cos mx = z_0\,e^{bt}$

$\cos mx$ ($z_0 \ll d$) on the interface separating two (immiscible, incompressible and inviscous) parallel concurrent flowing media ("lower" medium: velocity v_2, density ρ_2, small depth d; "upper" medium: velocity v_1, density ρ_1, infinite depth):

$$-b^2 = m^2c^2 = n^2 = \frac{\sigma m^3}{\rho_1 + \rho_2 \coth md} - \frac{g(\rho_1 - \rho_2)m}{\rho_1 + \rho_2 \coth md} - \frac{\rho_1\rho_2(\coth md)(v_2 - v_1)^2 m^2}{(\rho_1 + \rho_2 \coth md)^2} - \frac{2\sigma m}{D_w^2(\rho_1 + \rho_2 \coth md)}. \quad (5)$$

The influence of d can be simplified by taking $\coth md = 1/md$ for thin films; $\coth md = 1$ in case of $d = \infty$, i.e. for infinite depth of both media. Generally, $v_1 = 0$ is taken for convenience, cf. also the left-hand side of equation (1).

For applications to natural convection film boiling, various authors make use of simplifications of equation (5), which follow here:

Case (*i*).

$\rho_2 > \rho_1, \sigma = v_2 = 0, D_w = d = \infty$:

$$c^2 = -\frac{g}{m}\frac{\rho_1 - \rho_2}{\rho_1 + \rho_2} > 0, \quad (6)$$

i.e. in this case progressive waves of arbitrary wavelength along the originally horizontal flat interface are possible.

Case (*ii*). The case $\rho_2 < \rho_1$ (the lower medium has the lower density) is interesting for hydrodynamic stability of capillary waves in film boiling: $v_2 = 0, D_w = d = \infty$:

$$-\frac{b^2}{m^2} = c^2 = \frac{\sigma m}{\rho_1 + \rho_2} - \frac{g}{m}\frac{\rho_1 - \rho_2}{\rho_1 + \rho_2}. \quad (7)$$

According to Taylor [18], hydrodynamic stability of oscillations occurs only if $c > 0$, i.e. for wavelengths λ, which are shorter than the critical wavelength:

$$\lambda_c = \frac{2\pi}{m_c} = 2\pi\left[\frac{\sigma}{g(\rho_1 - \rho_2)}\right]^{\frac{1}{2}}. \quad (8)$$

The interface is unstable for $\lambda > \lambda_c$, as c and n are imaginary then. This implies a real exponent b, i.e. the ordinate shows an exponential growth. In film boiling, vapour flows continuously to the antinodes. The vapour is generated at those parts of the film boundary, where d is minimal i.e. instantaneously at the nodes (and at the lower part of the surface in case of a horizontal cylinder).

Case (*iii*). $\rho_2 < \rho_1, g = 0$ (formally; originally undisturbed vertical interface), $D_w = d = \infty$:

$$c^2 = \frac{\sigma m}{\rho_1 + \rho_2} - \frac{\rho_1\rho_2}{(\rho_1 + \rho_2)^2}(v_2 - v_1)^2. \quad (9)$$

This case of Helmholtz-instability, in which the relative upward velocity dominates, has been considered by Zuber [14, 15] to derive an expression for the nucleate boiling peak flux cf. equations (1) and (3).

Case (*iv*). $\rho_2 < \rho_1$, $D_w = \infty$, d: small (film boiling on a horizontal flat plate):

$$-\frac{b^2}{m^2} = c^2 = \frac{\sigma m}{\rho_1 + \rho_2/md} - \frac{g(\rho_1 - \rho_2)}{m(\rho_1 + \rho_2/md)} - \frac{\rho_1\rho_2 v_2^2}{(\rho_1 + \rho_2/md)^2\, md}. \quad (10)$$

This equation for combined Taylor–Helmholtz instability has been used by Berenson [21], who inserted into (10) an expression for the laminar vapour velocity v_2 (parallel to the plate) through the vapour film to the bubble space.

If $b = b(m) = b(\lambda)$ is real, the interface is unstable with a growing ordinate at an antinode of $z_0 e^{b(\lambda)t}$. The "most dangerous" or "dominant" unstable wavelength λ_d, which determines the bubble spacing at the Leidenfrost-point, corresponds to the maximum value of $b(m)$ following from differentiation of equation (7):

$$\lambda_d = \frac{2\pi}{m_d} = 2\pi\left[\frac{3\sigma}{g(\rho_1 - \rho_2)}\right]^{\frac{1}{2}} = \lambda_c\sqrt{3}. \quad (11)$$

Case (*v*). $\rho_2 < \rho_1$, $v_2 = 0$, $d = \propto$:

$$b^2 = -\frac{\sigma}{\rho_1 + \rho_2} m^3 + g\frac{\rho_1 - \rho_2}{\rho_1 + \rho_2} m + \frac{2\sigma}{D_w^2(\rho_1 + \rho_2)} m. \tag{12}$$

The case of film boiling on thin horizontal cylinders (heating wires) has been studied by Lienhard and Wong [22]. The influence of the circumferential surface tension is expressed in the last term on the right-hand side of equations (5) and (12). The dominant wavelength follows now from (12):

$$\lambda_d = \frac{2\pi\sqrt{3}}{\left[\frac{g(\rho_1 - \rho_2)}{\sigma} + \frac{1}{2R_w^2}\right]^{\frac{1}{2}}}, \tag{13}$$

where the cylinder radius $R_w = D_w/2$. The dominant wavelength is shortened in comparison to equation (11).

For very thin heating wires ($R_w \to 0$), (13) is simplified to:

$$\lambda_d = 2\pi R_w\sqrt{6} \tag{14}$$

i.e. λ_d is proportional to R_w and independent of liquid properties; i.e. for water at atmospheric pressure, the effect of R_w on λ_d dominates over the influence of the liquid properties for wires with $R_w < 2 \times 10^{-3}$ m. Equation (14) should thus be valid for the present investigations, where wires with $R_w = 10^{-4}$ m have been used.

Case (*vi*). $\rho_2 < \rho_1$, $v_2 = 0$:
Joosen [32] has shown, that the dominant wavenumber in this case of both a horizontal wire and a thin vapour film can be approximated by the following equation:

$$m_d = \frac{\rho_2}{3\rho_1 d} + \left[\left(\frac{\rho_2}{3\rho_1 d}\right)^2 + \frac{1}{3}\left\{\frac{g(\rho_1 - \rho_2)}{\sigma} + \frac{1}{2R_w^2}\right\}\right]^{\frac{1}{2}}. \tag{15}$$

Equation (15) is an extension, which approximates equation (13) as $d \to \propto$. The mean value of d can be taken here from the experimental boiling curve:

$$\bar{d} = \frac{h_2}{h_w} = \frac{k_2\theta_0}{q_w}. \tag{16}$$

The effect of a finite value of d is to shorten the dominant wavelength, similarly to the influence of the circumferential surface tension. Under the conditions of the present experiments, however, the effect of d on λ_d is restricted to only 2 per cent.

Case (*vii*). Ruckenstein [33] makes use of equation (7), and suggests that the bubble radius $R(t)$ at the Leidenfrost-point is proportional to:

$$\left(\frac{\sigma}{\rho_1 - \rho_2}\right)^{\frac{1}{2}} e^{bt}.$$

Case (*viii*). Frederking and Daniels [34] suggest, under the usual restriction to small perturbations, that the bubble period $\tau_d \sim 1/b_d$ and the departure radius $R_1 \sim 1/m_d$.

8.2 *Comparison with experimental data by others on pure liquids*

Most investigators assume, that the behaviour of adhering bubbles in film boiling at the Leidenfrost-point (which is practically independent of surface roughness [23]) is determined by hydrodynamic instability only. During each oscillation, a vapour bubble is generated alternately at the nodes and the antinodes.

8.2.1 *Horizontal plates and tubes.* Zuber [14, 15] makes use of equation (9) with $v_2 = 0$ at the Leidenfrost-point:

$$n^2 = \frac{\sigma m^3}{\rho_1 + \rho_2}. \tag{17}$$

The critical bubble period $\tau_c = 2\pi/n_c$ follows by inserting (8) into (17):

$$\tau_c = 2\pi\left[\frac{\rho_1 + \rho_2}{g(\rho_1 - \rho_2)}\right]^{\frac{1}{2}}\left[\frac{\sigma}{g(\rho_1 - \rho_2)}\right]^{\frac{1}{4}} \tag{18}$$

In accordance with Berenson's model [21], one can derive a similar expression from (17) for the dominant bubble period τ_d by inserting (11), which results in:

$$\tau_d/\tau_c = n_c/n_d = m_c^{\frac{3}{2}}/m_d^{\frac{3}{2}} = \lambda_d^{\frac{3}{2}}/\lambda_c^{\frac{3}{2}} = 3^{\frac{3}{4}},$$
$$\text{whence } \tau_d = 2{\cdot}28\ \tau_c.$$

Hosler and Westwater [35] measured the average bubble departure radius $\bar{R}_1$, the mutual distance between neighbouring sites generating bubbles, and the average bubble period $\bar{\tau}$ in water and Freon-11 on a horizontal aluminium heating plate at the minimum flux.

The average experimental values for water are: $\bar{R}_1 = 9{\cdot}4$ mm, which should be compared with $\lambda_c/4 = 3{\cdot}9$ mm and $\lambda_d/4 = 6{\cdot}8$ mm following from equations (8) and (11), respectively; the average spacing between neighbouring bubble centers amounts to 24·6 mm, cf. $\lambda_c = 15{\cdot}7$ mm and $\lambda_d = 27{\cdot}2$ mm; $\bar{\tau} = 0{\cdot}20$ s, cf. $\tau_c = 0{\cdot}10$ s and $\tau_d = 0{\cdot}23$ s following from equation (18).

The values for Freon-11 are: $\bar{R}_1 = 4{\cdot}4$ mm (cf. $\lambda_c/4 = 1{\cdot}8$ mm and $\lambda_d/4 = 3{\cdot}1$ mm); bubble spacing: 14·5 mm (cf. $\lambda_c = 7{\cdot}4$ mm and $\lambda_d = 12{\cdot}4$ mm); $\bar{\tau} = 0{\cdot}17$ s, cf. $\tau_c = 0{\cdot}07$ s and $\tau_d = 0{\cdot}16$ s. The extreme deviations from the average values amount to 25 per cent for R_1, to 100 per cent for the bubble spacing, and to 50 per cent for τ.

Obviously, Hosler and Westwater's average data are in good agreement with theoretical predictions based on the most dangerous wavelength λ_d. Support to Berenson's model is also given by experimental data of Kesselring, Roche and Bankoff [36] on transition and film boiling of Freon-113 on flattened horizontal steam-heated stainless steel tubes.

8.2.2 *Horizontal wires.* Lienhard and Wong [22] extended the hydrodynamic instability theory to the case of thin wires, cf. equations (12)–(14). The predicted $\lambda_d(R_w)$ is in good agreement with experimental data for isopropanol and benzene in film boiling on horizontal nichrome-V (60 µm $\leqslant R_w \leqslant$ 650 µm) wires and tungsten (25 µm $\leqslant R_w \leqslant$ 50 µm) wires. Also, $\lambda_d(q_w)$ has been measured.

More detailed results are: the measured λ_d (at constant R_w in isopropanol) is independent of q_w in the investigated range of 12 W/cm^2 to 50 W/cm^2 for $R_w = 60$ µm, and in the range 4 W/cm^2 to 15 W/cm^2 for $R_w = 250$ µm. The investigated heat fluxes are low, close to the Leidenfrost-point, to avoid the effect of bubble coalescence on λ_d. The measured λ_d exceeds in both liquids the theoretical value $\lambda_d = 2\pi R_w\sqrt{6}$, cf. equation (13), with 10 per cent, i.e. for thin wires the predicted independence of λ_d on liquid properties is in accordance with experimental data.

The predicted exponential growth of the ordinate $z = z_0\,e^{bt}$ at a node on the interface occurs below 0·53 λ_d in benzene and below 0·36 λ_d in isopropanol. These values are in good agreement with Lewis' [18] experimental limit of 0·4 λ.

Abadzic and Goldstein [37] report vapour removal from a horizontal platinum wire in columns or sheets for film boiling of carbon dioxide at pressures slightly below the critical. Above the critical point, similar free convection currents are observed.

9. PRESENT EXPERIMENTAL RESULTS IN FILM BOILING

9.1 *The boiling curves*

Boiling curves up to "burnout" (which is determined by local melting of the heating material) for water and for 4·1 wt % 2-butanone are shown in Figs. 1 and 2. *The ratio of the heat flux in the mixture to the corresponding value in water at the same average wire superheating (i.e. the ratio of the heat-transfer coefficients) in film boiling increases gradually from* 1·2 *at* $\theta_0 = 400°C$ *to* 1·8 *at* $\theta_0 = 1100°C$. This important result is in agreement with the abovementioned experimental data of Kautzky and Westwater [24] on the system carbon tetrachloride–Freon-113.

9.2 *The direct vapour production*

The vapour bubbles, which are released from the upper side of the vapour film surrounding the wire, are approximated by rotation ellipsoids with a vertical rotation axis. The bubble radius equals the radius of the equivalent sphere with the same volume. The total vapour volume $(4\pi/3)\sum_{0}^{\Delta t} R_1^3$, generated at the film interface during the interval Δt, has been measured from high-speed motion pictures taken at a rate of 3500 frames per s. The corresponding flux density is given by (cf. Table 1):

$$q_w{}^* = \frac{4\pi}{3}\,\frac{\rho_2 l}{\Delta t}\,\frac{\sum_{0}^{\Delta t} R_1^3}{\pi D_w L_w}. \tag{19}$$

For these experiments, Δt amounted to approximately 200 ms. The volume of bubbles adhering at $t = 0$ is subtracted, and the corresponding volume at $t = \Delta t$ is added to the sum on the right-hand side of equation (19).

The radiant flux density has been calculated from the Stefan–Boltzmann law:

$$q'_w = 5{\cdot}67 \times 10^{-8}\,\varepsilon_w(T_w^4 - T^4), \tag{20}$$

where $T_w = T + \theta_0$ and T denote absolute temperatures. Absorption of radiation in the vapour film has been neglected. Corresponding to the wire superheating shown in Table 1, the following values of the emissivity ε_w for platinum wires have been used [29]: $\varepsilon_w = 0{\cdot}085$ at $T_w = 681$ K ($\theta_0 = 329$°C, ethanol, I); $\varepsilon_w = 0{\cdot}133$ at $T_w = 1117$ K ($\theta_0 = 744$°C, water, I); $\varepsilon_w = 0{\cdot}138$ at $T_w = 1148$ K ($\theta_0 = 788$°C, mixture); $\varepsilon_w = 0{\cdot}142$ at $T_w = 1183$ K ($\theta_0 = 831$°C, ethanol, II); $\varepsilon_w = 0{\cdot}165$ at $T_w = 1436$ K; ($\theta_0 = 1063$°C, water, II). $\varepsilon_1 = 0{\cdot}96 \approx 1$ for water at atmospheric boiling point.

It may be worth noticing, that in calculating $q_w{}^*$, cf. equation (19), for the mixture, the numerical values of ρ_2 and l for saturated steam at atmospheric pressure have been used. If interpolated values between those of pure water and 2-butanone should have been inserted, according to the relative volatility of the organic component, even a lower $q_w{}^*$ is calculated, down to a factor of 0·8 in case of pure 2-butanone.

The most interesting experimental results are, cf. Table 1:

(i) *The direct vapour production at the film in pure liquids (water and ethanol) accounts to 95 per cent of the total heat flux diminished with the small radiant flux.*

(ii) *Contrarily, in 4·1 wt % 2-butanone, the contribution of the direct vapour production is reduced to 53 per cent.*

Result (i) is obvious. The observed average deviation of only 3 per cent in water, (I, II), and ethanol, (I), justifies the approximation of the actual bubble shape at departure to a rotation ellipsoid (Figs. 3–5). The larger deviation of 10 per cent in ethanol, (II), is due to bubble coalescence. Result (i) shows also, that the convective currents arising from the heated bottom plate of the boiling vessel have no appreciable influence on the direct vapour production at the wire.

Result (ii) is in agreement with previous observations in nucleate boiling [8–10]. Apparently, approximately 50 per cent of the total heat flux, which is transmitted through the vapour film, is directed to the bulk liquid.

9.3 *Behaviour of individual vapour bubbles*

The average number of prominences on the vapour film around the wire, from which bubbles originate, is shown in Table 1. For water, this number is only slightly dependent on heat flux (Figs. 3 and 4); in ethanol a considerable decrease at increasing heat flux occurs, which is due to the coalescence of neighbouring bubbles. At least partly for the same reason, the average bubble departure diameter increases with increasing heat flux; this effect is most pronounced also in ethanol (Table 1). In addition, the average bubble frequency on a prominence decreases.

Figure 6—water (I, II)— and Fig. 7—4·1 wt % 2-butanone—show the growth of individual vapour bubbles during adherence and after

departure. The investigated bubbles show no coalescence and their individual frequency equals the average value for approximately 50 bubbles in each liquid (cf. Tables 1 and 2).

Apparently, bubble departure is associated with a sudden decrease in the radius (Figs. 6 and 7), which is due to the circumstance that the vapour in the lower part of the bubble space is covered then with saturated liquid. This indicates a previous superheating of the vapour in the bubble. The instantaneous condensation at departure causes bubble oscillations about the spherical shape especially in water (Fig. 6). In ethanol, bubble oscillations occur already during adherence.

The bubble departure time, t_1, is approximately independent of the liquid composition (Table 2). The waiting time, t_2, equals the departure time in water, (II), and in 4·1 wt % 2-butanone; this is in accordance with predictions of the theoretical models for film boiling based on hydrodynamic instability of harmonic surface waves, cf. [14, 15, 21, 22].

The observed short waiting time ($t_2 = 5$–6 ms) in ethanol is striking. Possibly, this may be related to the oscillation period of the investigated bubbles during adherence: relative maxima and minima occur in the growth curve $R(t)$ during adherence at time intervals of (5 ± 1) ms, Fig. 8. Generally, bubble oscillations

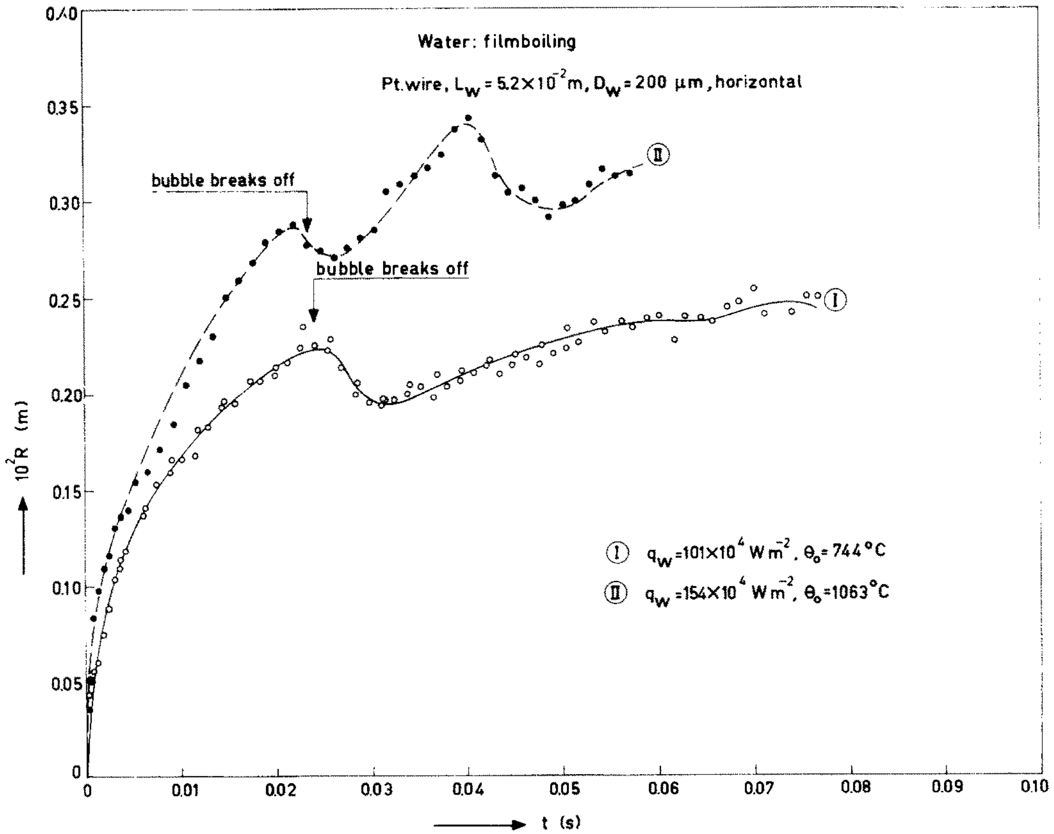

FIG. 6. Water, (I) and (II). Growth curves for individual vapour bubbles during adherence to the film and after release, cf. Figs. 1, 3 and 4.

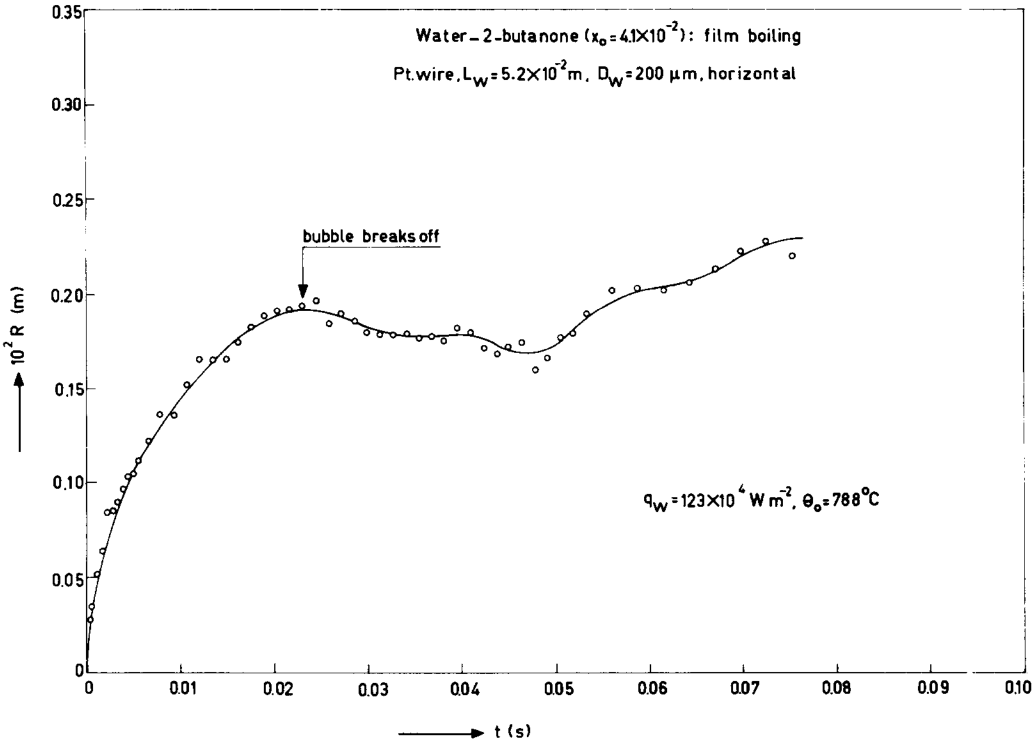

FIG. 7. 4·1 wt % 2-butanone in water, (I). Growth curve for individual vapour bubble during adherence to the film and after release, cf. Figs. 2 and 5.

in boiling are caused by coalescence [6, 7]. Bubbles grow not only during adherence, but also after departure (Figs. 6 and 7); this is obviously due to a relatively small superheating of the bulk liquid, cf. [6].

10. COMPARISON WITH THEORY

10.1 *Influence of the dominant wavelength*

A comparison of the experimental data on the bubble departure radius and the bubble spacing with theoretical predictions based on the dominant wavelength, λ_d, is obvious. Apparently however, one may expect a more complicated situation at the higher heat fluxes used in our experiments (corresponding to larger direct vapour productions at the film) than at the minimum heat flux in film boiling. In this respect, it may be worth noticing, that the property constants of the investigated liquids differ considerably from the values of isopropanol and benzene, which have been used by Lienhard and Wong [22], as mentioned previously.

Table 3 shows the experimental $4\bar{R}_1$ and the twofold of the bubble spacing, $2\bar{L}$, which should equal λ_d (or λ_c) derived from equation (13) for horizontal heating wires, or λ_d (or λ_c) following from equations (8) and (11) for horizontal plates.

Actually, one finds for the theoretical λ_d = 1·53 mm following from equation (14) for wires with a diameter of 0·200 mm (independent of liquid properties); $\lambda_d < 2\bar{L} < 4\bar{R}_1$. One should be inclined to suppose, that Lienhard and Wong's theoretical model, which is valid for the conditions at the Leidenfrost-point, fails completely at high heat fluxes of the wire.

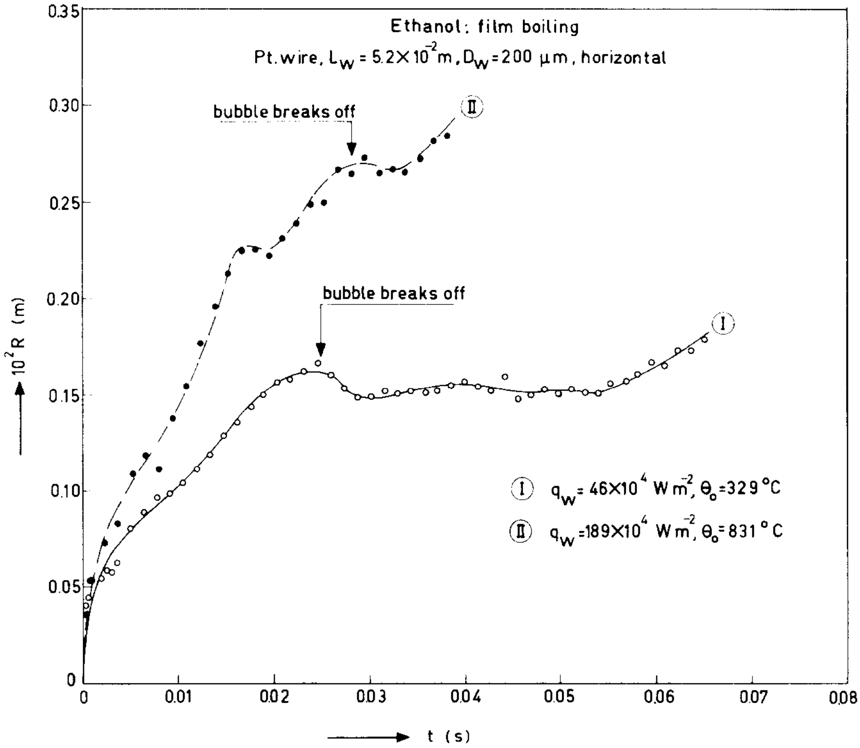

FIG. 8. Ethanol, (I) and (II), cf. Table 1. Growth curves for individual vapour bubbles during adherence to the film and after release.

However, accurate inspection of the motion pictures, especially for ethanol, (I), with the lowest wire superheating investigated, cf. Table 1, shows that a limited number of prominences with $2\bar{L} = \lambda_d$ are present on the vapour film (Fig. 3–5). Lienhard and Wong [22] made the same observation at higher heat fluxes. Obviously, at increasing heat flux the original regular pattern is disturbed, not only by bubble coalescence, but also by coalescence of neighbouring prominences, i.e. already during the initial stage of bubble growth.

In absence of coalescence, one expects in the following expression:

$$\bar{L} = \beta \frac{\lambda_d}{2} \tag{21}$$

Table 2. Departure time, t_1, waiting time, t_2, frequency ν, and departure radius, R_1, of individual bubbles in film boiling on horizontal platinum wire, cf. Table 1 and Figs. 6 and 7

Liquid		t_1 (ms)	t_2 (ms)	$t_1 + t_2$ (ms)	$\nu = 1/(t_1 + t_2)$ (1/s)	t_2/t_1	R_1 (mm)	$\bar{R}_1$ (mm)
Water	(I)	24	14	38	26	0·58	2·23	2·34
	(II)	23	22	45	22	0·96	2·51	2·87
Ethanol	(I)	25	5	30	33	0·20	1·60	1·52
	(II)	28	6	34	29	0·21	2·71	3·17
4·1 wt % 2-butanone		23	21	43	23	0·91	1·96	2·11

Table 3. Experimental average bubble departure radius, $\bar{R}_1$, and bubble spacing in film boiling, in comparison to theoretical predictions based on hydrodynamic instability

Horizontal platinum wire, $D_w = 200\ \mu m$, $L_w = 5{\cdot}2$ cm	Water (I)	Water (II)	Water–2-butanone ($x_0 = 4{\cdot}1 \times 10^{-2}$)	Ethanol (I)	Ethanol (II)
Present experiments					
$4\bar{R}$ (mm)	9·36	11·48	8·44	6·04	12·68
2 (bubble center distance) (mm)	6·12	6·50	5·68	4·72	9·46
Theory					
Lienhard and Wong [22] equation (13)					
λ_c (mm)	0·88		0·88	0·88	
m_c (mm^{-1})	7·08		7·09	7·10	
λ_d (mm)	1·53		1·53	1·53	
m_d (mm^{-1})	4·09		4·09	4·10	
Zuber [14, 15] equation (8)					
λ_c (mm)	15·7		13·2	9·8	
m_c (mm^{-1})	0·400		0·475	0·639	
Berenson [21] equation (11)					
λ_d (mm)	27·2		22·8	17·0	
m_d (mm^{-1})	0·231		0·274	0·369	

Table 4. Ratio of experimental average bubble spacing and departure radius in film boiling, in comparison to the theoretical λ_d, cf. equation (13)

Horizontal platinum wire, $D_w = 200\ \mu m$, $\lambda_d = 1{\cdot}53$ mm	Water (I)	Water (II)	Water–2-butanone ($x_0 = 4{\cdot}1 \times 10^{-2}$)	Ethanol (I)	Ethanol (II)
$\beta = 2\,\bar{L}/\lambda_d$	4·00	4·25	3·71	3·08	6·18
$2\,\bar{R}_1/\bar{L}$	1·53	1·77	1·48	1·49	1·34
$4\,\bar{R}_1/\lambda_d$	6·12	7·50	5·52	3·95	8·29

a theoretical value of $\beta = 1$, for wires with $D_w = 0{\cdot}20$ mm, if $\lambda_d = 1{\cdot}53$ mm is inserted. The comparable values involving coalescence at high heat fluxes follow from the data of Table 3: $\beta = 4$ both in water and the mixture, and $\beta = 3$ and $\beta = 6$, respectively, in ethanol (these values have been rounded off slightly, cf. Table 4). β is expected to be a positive integer; even numbers denote coalescence of an odd number of neighbouring bubbles, odd numbers involve coalescence of an even number of neighbouring bubbles.

The ratio of the average bubble departure diameter, $2\bar{R}_1$, to the bubble center distance, $\bar{L}$, amounts to (Table 4) 1·6 in water and the mixture, and to 1·4 in ethanol, i.e. in general to 1.5. The ratio of the twofold of the departure diameter to λ_d amounts to 7 in water, to 5·5 in the mixture, and increases with increasing heat flux from 4 to 8 in ethanol. In the latter liquid, $\bar{L}$ increases also considerably then.

10.2 *The burnout flux density*

10.2.1 *Water*. The experimental burnout of the wires (diameter: $2{\cdot}00 \times 10^{-4}$ m) occurs both in water and the investigated mixture at an average superheating of $\theta_0 = 1160$°C, (corresponding to $T_w = 1580$ K), cf. Figs. 1 and 2. This value is considerably below the melting point of platinum, which occurs apparently only locally, partly due to an end-effect on the wire. The burnout heat flux density in water (185×10^4 W/m^2, Fig. 1, i.e. 2·5 times the nucleate boiling peak flux) is assumed to equal the direct vapour production rate at the film (Table 1).

If the vapour removal from the film is supposed to be limited by a Helmholtz instability—according to Zuber's model [14, 15], cf. equations (1) and (2)—, the critical upward vapour velocity is given by:

$$v_{2,c} = \left[\frac{\rho_1 \sigma m_c}{\rho_2(\rho_1 + \rho_2)}\right]^{\frac{1}{2}}. \qquad (22)$$

Similarly to equations (3) and (2), the corresponding burnout flux density for $m_c = 400$ m^{-1} (Table 3) should be given by:

$$\begin{aligned}185 \times 10^4\ \mathrm{W/m^2} &= f \rho_2 l v_{2,c} \\ &= f \rho_2 l \left[\frac{\rho_1 \sigma m_c}{\rho_2(\rho_1 + \rho_2)}\right]^{\frac{1}{2}} \\ &= f\, l\, [\sigma g(\rho_1 - \rho_2)]^{\frac{1}{4}} \left(\frac{\rho_1 \rho_2}{\rho_1 + \rho_2}\right)^{\frac{1}{2}} \\ &= f.\, 850 \times 10^4\ \mathrm{W/m^2}. \qquad (23)\end{aligned}$$

The constant of proportionality $f = 0{\cdot}22$ for water denotes the fraction occupied by the vapour columns, cf. Zuber's factor $f = \pi/24 = 0{\cdot}13$ for the nucleate boiling peak flux on a horizontal plate. The critical upward vapour velocity $v_{2,c} = 6{\cdot}2$ m/s, and the corresponding downward liquid velocity $v_{1,c} = -(\rho_2/\rho_1)\, v_{2,c} = 4 \times 10^{-3}$ m/s.

10.2.2 *Mixture.* 4·1 wt % 2-butanone. One has for this mixture, where $m_c = 475$ m^{-1} (Table 3): $f = 0{\cdot}53 \times 340 \times 10^4/890 \times 10^4 = 0{\cdot}20$. The factor of 0·53 is taken from Table 1, the burnout flux density of 340×10^4 W/m^2 is shown in Fig. 2; the direct vapour production rate amounts here to $0{\cdot}53 \times 340 \times 10^4$ W/m^2 $= 180 \times 10^4$ W/m^2.

10.2.3 *Conclusions. The quantitative agreement at burnout of both the average wire temperature, the direct vapour production rate, and the fraction occupied by the vapour columns in water and in 4·1 wt % 2-butanone is very satisfactory.* This situation is similar to the conditions at the nucleate boiling peak flux, where equal vapour production rates occur also at the same wire temperature, as mentioned previously [8–10]. Both in nucleate boiling and in film boiling, considerably higher maximum heat fluxes occur in the mixture. The maximum vapour production rate in film boiling exceeds the value in nucleate boiling with a factor of 6. At present, these statements are restricted to a special geometry; the effect of the melting point on the burnout flux has not been studied until now.

11. EXPLANATION OF THE EFFECT OF MASS DIFFUSION IN MIXTURES

11.1 *The increase in heat flux*

The increased values of the heat-transfer coefficient occurring in film boiling of 4·1 wt % 2-butanone in comparison to water, are explained as follows: the previously observed slowing down of the growth rate of both free and adhering bubbles in nucleate boiling at a certain (low) concentration of the more volatile component is ultimately due to an increase of the boiling temperature of the liquid at the bubble boundary. This increase is caused by a lower local concentration of the more volatile component near the boundary, which is in thermodynamic equilibrium with a considerably higher concentration in the vapour.

Similarly, the vaporization rate of liquid at the interface of the vapour film in film boiling is diminished by an exhaustion of the more volatile component in an adjacent thin (mass diffusion) liquid layer with an ultimate thickness of $2(Dt_2)^{\frac{1}{2}} = 2(Dt_1)^{\frac{1}{2}}$. At burnout, a complete local exhaustion of the more volatile component may be expected to occur, which causes a maximum superheating of the adjacent liquid layer of $\theta_{0,1} = 11$°C (i.e. the difference in atmospheric boiling point between water and the mixture). The corresponding average maximal heat flux density, which is directed into the bulk liquid of the mixture, amounts to:

$$\bar{q}_{1,\max} = \frac{1}{t_1}\int_0^{t_1} \frac{k_1 \theta_{0,1}}{2(Dt)^{\frac{1}{2}}}\, \mathrm{d}t = \frac{k_1 \theta_{0,1}}{(Dt_1)^{\frac{1}{2}}}. \qquad (24)$$

For 4·1 wt % 2-butanone at burnout, $\bar{q}_{l,\max} = 157 \times 10^4\,\mathrm{W/m^2}$, if $t_1 = t_2 = 22$ ms (Table 2) is taken in equation (24). This value is in quantitative agreement with the maximal experimental value of $q_w - q_w{}^* - q'_w = (340 - 180 - 4)\,10^4\,\mathrm{W/m^2} = 156 \times 10^4\,\mathrm{W/m^2}$ (cf. Fig. 2 and Table 1).

At increasing wire superheating in film boiling, a gradual increase in both $\theta_{0,1}$ and $\bar{q}_1$ is expected, also in accordance with the experimental results. It may be worth noticing, that the derivation of equation (24) is independent of the location at the outer film interface, and consequently also practically independent of the geometry of the heating surface, cf. the experimental results on a horizontal flat plate presented in [23, 24].

11.2 *Bubble growth during adherence*

At present, theoretical insight is lacking to describe the behaviour of individual vapour bubbles at high wall superheatings in film boiling, which are of considerable practical importance. By conversion of the reasoning presented in the preceding Section, equation (24) delivers an expression for the adherence time, t_1, and thus also for the bubble frequency. Obviously, the numerical values, which are derived in this way, are in agreement with the experimental values (Table 2).

Generally, the individual bubble growth at high fluxes is complicated by coalescence. Even in absence of coalescence, the mechanism governing individual growth is not well understood at present. Inspection of the growth curves for bubbles in water (Fig. 6) suggest a behaviour, which is similar to that of free bubbles [4–10], where the asymptotic growth is controlled by heat diffusion only:

$$R(t) = C\,\theta_{0,1}t^{\frac{1}{2}}. \tag{25}$$

For saturated water at atmospheric pressure, $C = 24 \times 10^{-4}\,\mathrm{ms^{-\frac{1}{2}}\,{}^\circ C^{-1}}$, which corresponds to an effective liquid superheating of $\theta_{0,1} = 6$°C for water, (I), and to $\theta_{0,1} = 8$°C for water, (II). For ethanol, with $C = 9 \times 10^{-4}\,\mathrm{ms^{-\frac{1}{2}}\,{}^\circ C^{-1}}$, $\theta_{0,1} = 16$°C has been calculated previously [6]. In the investigated mixture, the situation is complicated by the instantaneous additional liquid superheating due to concentration differences, cf. Section 11.1. This attributes to a faster bubble growth in the mixture as the value of $C = 6 \times 10^{-4}\,\mathrm{ms^{-\frac{1}{2}}\,{}^\circ C^{-1}}$ [6, 7] suggests, cf. Figs. 6 and 7. As mentioned previously, the vapour feeding the bubble space must be superheated to a certain degree, at least initially. This implies also a superheating of an adjacent liquid layer.

Our future research programme includes recordings of local temperature fluctuations in film boiling with the main purpose of studying the mechanism, which underlies bubble growth at high heat fluxes. Similar investigations on adhering bubbles in nucleate boiling have been carried out recently [11].

12. SURVEY

Film boiling of water and of an aqueous binary mixture with a more volatile component (4·1 wt % 2-butanone) has been studied on a horizontal, electrically heated platinum wire with a diameter of 200 μm.

In nucleate boiling of water—2-butanone, the investigated mixture shows a previously observed coincidence of a maximum peak flux and a minimum growth rate of vapour bubbles ("boiling paradox"). The slowing down of bubble growth is due to mass diffusion of the more volatile component.

Present experimental results for the mixture, i.e. both a (to 50 per cent) decreased direct vaporization rate at the vapour film, and an in comparison to water increased heat flux (up to with a factor of 1·8) at constant wire superheating up to burnout, indicate a similar effect of mass diffusion in film boiling of binaries.

A survey is given of the current theories on film boiling (which are based on hydrodynamic instability of the vapour–liquid interface, and on the mechanism of heat removal from the surface, respectively), and of the various modifications. Experimental data on bubble behaviour are compared to theoretical predictions involving the dominant wavelength. The effect of coalescence at high heat fluxes has been studied.

The observed influence of mass diffusion in film boiling of the mixture has been explained analogously to nucleate boiling: a local exhaustion of the more volatile component at the film interface establishes a temperature gradient in an adjacent liquid layer. This gradient causes a heat flow in the direction of the bulk liquid.

ACKNOWLEDGEMENT

The authors are indebted to Professor R. Cole of Clarkson College of Technology, Potsdam, N.Y., U.S.A., on sabbatical leave at the University of Technology, Eindhoven, for valuable comments on the manuscript.

REFERENCES

1. W. R. van Wijk, A. S. Vos and S. J. D. van Stralen, Heat transfer to boiling binary liquid mixtures, *Chem. Engng Sci.* **5**, 68–80 (1956).
2. S. J. D. van Stralen, Warmteoverdracht aan kokende binaire vloeistofmengsels (Heat transfer to boiling binary liquid mixtures). Doctor thesis. University of Groningen, Netherlands; Veenman, Wageningen, Netherlands (1959); *Meded. Landbouw-Hoogesch. Wageningen* **59** (6), 1–82 (1959). In Dutch with English summary and captions.
3. S. J. D. van Stralen, Heat transfer to boiling liquid mixtures, *Br. Chem. Engng* **4**, 8–17 (1959); **4**, 78–82 (1959); **6**, 834–840 (1961); **7**, 90–97 (1962).
4. L. E. Scriven, On the dynamics of phase growth, *Chem. Engng Sci.* **10**, 1–13 (1959).
5. P. J. Bruijn, On the asymptotic growth rate of vapour bubbles in superheated binary liquid mixtures, *Physica 'sGrav.* **26**, 326–334 (1960).
6. S. J. D. van Stralen, The growth rate of vapour bubbles in superheated pure liquids and binary mixtures. Part I: Theory. Part II: Experimental results, *Int. J. Heat Mass Transfer* **11**, 1467–1490, 1491–1512 (1968).
7. S. J. D. van Stralen, Bubble growth rates in boiling binary mixtures, *Br. Chem. Engng* **12**, 390–394, 143–147, (1967).
8. S. J. D. van Stralen, The mechanism of nucleate boiling in pure liquids and in binary mixtures, Parts I–IV, *Int. J. Heat Mass Transfer* **9**, 995–1020, 1021–1046 (1966); **10**, 1469–1484, 1485–1498 (1967).
9. S. J. D. van Stralen, The boiling paradox in binary liquid mixtures. *Chem. Engng Sci.* **25**, 149–171 (1970).
10. S. J. D. van Stralen, On the mechanism of nucleate boiling in binary systems. *Abstracts of papers and communications of the third-all union heat and mass transfer conference*, Minsk, 67–68, 256 (1968); *Proceedings* 2, 219–243 (1968). In Russian.
11. S. J. D. van Stralen and W. M. Sluyter, Local temperature fluctuations in saturated pool boiling of pure liquids and binary mixtures, *Int. J. Heat Mass Transfer* **12**, 187–198 (1969).
12. A. S. Vos and S. J. D. van Stralen, Heat transfer to boiling water–methylethylketone mixtures, *Chem. Engng Sci.* **5**, 50–56 (1956).
13. S. J. D. van Stralen and W. M. Sluyter, Investigations on the critical heat flux of pure liquids and mixtures under various conditions, *Int. J. Heat Mass Transfer* **12**, 1353–1384 (1969).
14. N. Zuber, On the stability of boiling heat transfer, *Trans. Am. Soc. Mech. Engrs* **80**, 711–720 (1958).
15. N. Zuber and M. Tribus, Further remarks on the stability of boiling heat transfer, Rep. 58–5, Dept. of Engng. Univ. of California, Los Angeles (1958).
16. L. S. Tong, *Boiling Heat Transfer and Two-Phase-Flow*, Wiley, New York (1965).
17. M. T. Cichelli and C. F. Bonilla, Heat transfer to liquids boiling under pressure, *A.I. Ch. E. Jl* **41**, 755–787 (1945).
18. G. Taylor, The instability of liquid surfaces when accelerated in a direction perpendicular to their plane. Part I, *Proc. R. Soc.* **201A**, 192–196 (1950); D. J. Lewis, Part II, *Proc. R. Soc.* **202A**, 81–96 (1950).
19. L. A. Bromley, Heat transfer in stable film boiling, *Chem. Engng Prog.* **46**, 221 (1950).
20. Y. P. Chang, A theoretical analysis of heat transfer in natural convection and in boiling, *Trans. Am. Soc. Mech. Engrs* **79**, 1501–1513 (1957); Wave theory of heat transfer in film boiling, *J. Heat Transfer* **81**, 1–12 (1959).
21. P. J. Berenson, Film-boiling heat transfer from a horizontal surface, *J. Heat Transfer* **83**, 351–358 (1961).
22. J. H. Lienhard and P. T. Y. Wong, The dominant unstable wavelength and minimum heat flux during film boiling on a horizontal cylinder, *J. Heat Transfer* **86**, 220 (1964).
23. D. P. Jordan, Film and transition boiling, *Advances in Heat Transfer*, edited by T. F. Irvine and J. P. Hartnett, Vol. 5, pp. 55–128 Academic Press, New York (1968).
24. D. E. Kautzky and J. W. Westwater, Film boiling of a mixture on a horizontal plate, *Int. J. Heat Mass Transfer* **10**, 253–256 (1967).
25. T. Dunskus and J. W. Westwater, The effect of trace additives on the heat transfer to boiling isopropanol, *Chem. Engng Prog. Symp. Ser.* 32, **57**, 173–180 (1961).
26. W. Nusselt, Die Oberflächenkondensation des Wasserdampfes, *Z. VDI* **60**, 541–546, 569–575 (1916).
27. H. Gröber, S. Erk and U. Grigull, *Die Grundgesetze der Wärmeübertragung*, 3rd ed. Springer-Verlag, Berlin (1961).
28. P. Pitschmann and U. Grigull, Filmverdampfung an waagerechten Zylindern, *Wärme und Stoffübertragung* **3**, 75–84 (1970).
29. C. D. Hodgman, *Handbook of Chemistry and Physics*, 43rd ed. Chemical Rubber, Cleveland (1961).
30. H. Lamb, *Hydrodynamics*, 6th ed. University Press, Cambridge (1957).

31. L. M. MILNE-THOMPSON, *Theoretical Hydrodynamics*, 3rd ed. Macmillan, New York (1955).
32. C. J. J. JOOSEN, Heat transfer in film boiling and in forced cirulation of water and a binary mixture, Engineer Thesis, Technological University, Eindhoven, Netherlands (1970). In Dutch.
33. E. RUCKENSTEIN, Film boiling on a horizontal surface, *Int. J. Heat Mass Transfer* **10**, 911–919 (1967).
34. T. H. K. FREDERKING and D. J. DANIELS, The relation between bubble diameter and frequency of removal from a sphere during film boiling, *J. Heat Transfer* **88**, 87–93 (1966).
35. E. R. HOSLER and J. W. WESTWATER, Film boiling on a horizontal plate, *ARS Jl* **32**, 553–558 (1962).
36. R. C. KESSELRING, P. H. ROSCHE and S. G. BANKOFF, Transition and film boiling from horizontal strips, *A.I. Ch. E. Jl* **13**, 669–675 (1967).
37. E. ABADZIC and R. J. GOLDSTEIN, Film boiling and free convection heat transfer to carbon dioxide near the critical state, *Int. J. Heat Mass Transfer* **13**, 1163–1175 (1970).

EBULLITION EN FILM DE L'EAU ET D'UN MELANGE BINAIRE AQUEUX

Résumé—L'ébullition en film de l'eau et d'un mélange binaire aqueux avec un composant plus volatile (4,1 % en poids 2-butanone) a été étudiée sur un fil de platine horizontal chauffé électriquement et ayant 200 µm de diamètre.

Le résultat expérimental le plus important pour le mélange est la réduction de la production directe de vapeur dans le film laquelle concerne seulement 53% du flux thermique, en opposition avec la valeur de 95% dans les liquides purs. En outre le coefficient de transfert thermique dans le mélange est augmenté jusqu'à un facteur de 1,8 à la caléfaction, en comparaison avec l'eau.

Le comportement surprenant du mélange est attribué à la diffusion massique: un enrichissement local dû composant le plus volatile dans le liquide à l'interface du film provoque un flux thermique additionnel dans le noyau liquide.

FILMSIEDEN VON WASSER UND EINEM WÄSSRIGEN ZWEISTOFFGEMISCH

Zusammenfassung—Filmsieden von Wasser und einem wässrigen Zweistoffgemisch mit einer flüchtigeren Komponente (4,1 Gew.% z-Butanon) wurde an horizontalen, elektrisch beheizten Platindrähten mit einem Durchmesser von 200 µm untersucht. Das wichtigste Versuchsergebnis ist die Verminderung der direkten Dampferzeugung am Film in der Mischung, die nur noch 53 Prozent des Wärmeflusses ausmacht im Gegensatz zu 95 Prozent bei reinen Flüssigkeiten.

Die Wärmeübergangszahl wurde in der Lösung beim burn-out um einen Faktor 1,8 gesteigert im Vergleich zu Wasser.

Das merkwürdige Verhalten in der Lösung wird der Massen-Diffusion zugeschrieben: ein lokaler Ausstoss der leichter flüchtigen Komponente an der Filmgrenze ruft einen zusätzlichen Wärmestrom, in die Flüssigkeit hinein, hervor.

ПЛЕНОЧНОЕ КИПЕНИЕ ВОДЫ И БИНАРНОЙ СМЕСИ

Аннотация—Исследовалось пленочное кипение воды и бинарной смеси с более летучим компонентом (4,1% 2–бутанон) на горизонтальной нагреваемой электричеством платиновой проволоке диаметром 200 мм. Наиболее важным экспериментальным результатом явилось обнаруженное снижение прямого парообразования на пленке смеси, которое составляет только 53% теплового потока, тогда как для чистых жидкостей оно равно 95%. Кроме того найдено, что коэффициент теплообмена для смеси в критической точкё увеличивается по сравнению с водой в 1,8 раз. Необычное поведение смеси объясняется диффузией массы: локальное истечение более летучего компонента жидкости на границе раздела дленки вызывает дополнительный тепловой поток в объём жидкости.